Journal of Physics A:
Mathematical and Theoretical

PAPER

Improved reduced order model for study of coupled phenomena

To cite this article: Shubham Garg and Kirankumar R Hiremath 2024 *J. Phys. A: Math. Theor.* **57** 415202

IOP Publishing Journal of Physics A: Mathematical and Theoretical
J. Phys. A: Math. Theor. **57** (2024) 415202 (22pp) https://doi.org/10.1088/1751-8121/ad7ca1

Improved reduced order model for study of coupled phenomena

Shubham Garg and Kirankumar R Hiremath*

Department of Mathematics, Indian Institute of Technology Jodhpur, Jodhpur, Rajasthan 342030, India

E-mail: k.r.hiremath@iitj.ac.in and garg.14@iitj.ac.in

Received 13 March 2024; revised 5 September 2024
Accepted for publication 18 September 2024
Published 26 September 2024

Abstract

Many interesting phenomena in applications are based on interactions between their constituent sub-systems. The first principle exact models of these phenomena can be quite complicated. Therefore, many practitioners prefer to use so-called phenomenological models, which are generally known as models based on coupled mode theory (CMT). This type of reduced-order model captures the dominant behavior of the system under appropriate conditions. Quite often, these validity conditions are qualitatively described, but no detailed mathematical analysis is provided. This work addresses this issue and presents improvements in the traditional phenomenological models. Although an LC circuit model is used for illustration due to its simplicity, the results in this work are equally applicable to a wide variety of coupled models. A detailed mathematical analysis is carried out to quantify the order of approximation involved in the model-based CMT. Using it, the validity of the model in the regime from weak coupling to strong coupling is analytically investigated. An improved reduced-order model is proposed, which gives better results than the traditional phenomenological model. The analytical studies are verified with numerical simulations, which clearly show better validity of the proposed improved model of coupled systems.

Keywords: coupled oscillators, coupled mode theory, Hamiltonian method, canonical transformation

1. Introduction

In a coupled phenomenon, the dynamics of one component of the system affect the dynamics of the rest. Many physical systems, such as waveguide couplers, resonance circuits, and oscillators, involve coupling between two or more sub-systems [13, 19]. To understand such

* Author to whom any correspondence should be addressed.

systems completely, one needs to solve a coupled system of differential equations with proper initial and boundary conditions. However, such a system often lacks analytic solutions, and direct numerical simulation can be time-consuming. Therefore, many practitioners prefer to use so-called phenomenological models, which capture the dominant behavior of the system under appropriate conditions.

Without loss of generality, we assume that the system under consideration is formed by coupling the two sub-systems. In practice, the coupled mode theory (CMT) is frequently used to explain the interactions between constituent sub-systems [13]. It is a general phenomenological approach that helps understand the interaction between the normal modes of two systems that are coupled to each other [7, 16]. There are some assumptions and approximations used in CMT.

There are two variants of CMT: one is the coupling of modes in the space domain that Yariv introduced [31], and the other is the coupling of modes in the time domain that Pierce introduced [24]. Refer [14, 28] for the difference between the spatial CMT and temporal coupled-mode theory (TCMT). An early review of the two can be found in [14]. In this study, we use the coupling of the modes in the time domain.

Consider two systems, each having only one normal mode of dynamics. Suppose these systems are not coupled. Then their normal modes will evolve with their natural frequencies ω_1 and ω_2, which can be modeled mathematically by the system of differential equations

$$\begin{aligned} \frac{\mathrm{d}a_1}{\mathrm{d}t} &= j\omega_1 a_1, \\ \frac{\mathrm{d}a_2}{\mathrm{d}t} &= j\omega_2 a_2. \end{aligned} \tag{1}$$

Here $j = \sqrt{-1}$ and $a_1(t), a_2(t)$ are the eigenfunctions corresponding to the eigenvalues ω_1, ω_2 of the two uncoupled systems. If we assume the coupling between two modes is 'weak', i.e. the dynamics of the uncoupled modes are 'weakly' modified, then the interaction between the two modes can be phenomenologically given by [13]

$$\begin{aligned} \frac{\mathrm{d}a_1}{\mathrm{d}t} &= j\omega_1 a_1 + \kappa_{12} a_2, \\ \frac{\mathrm{d}a_2}{\mathrm{d}t} &= \kappa_{21} a_1 + j\omega_2 a_2. \end{aligned} \tag{2}$$

The equation (2) describes the weak coupling between two modes of a coupled system in the time domain. The parameters κ_{12}, κ_{21} show the effect of coupling of mode 2 on mode 1 and vice-versa, respectively. Thus, CMT is a general procedure describing many coupled systems [13]. Note that equation (2) is a phenomenological-based approach model. In addition to its computational benefits, CMT provides the opportunity to learn valuable physical understanding by examining the simpler ordinary differential equations that arise and carefully evaluating the impact of each term or phenomenon by manually turning it on or off [3].

The literature on CMT is very vast. Pierce first introduced CMT for the analysis of microwave traveling-wave tubes [24]. Gould used the CMT for the analysis of the backward-wave oscillator [11]. Miller and Louisell used the CMT approach to analyze microwave waveguides and tapered waveguide structures, respectively [18, 22].

Usually, three conditions are used in CMT equations: energy conservation, time-reversal symmetry, and reciprocity. Energy conservation refers to the principle that the total energy of the coupled system remains constant. The energy can only be transferred between two systems that are coupled. From a mathematical perspective, the principle of energy conservation can

be understood as a closed-orbit solution. The time-reversal symmetry can be interpreted as the system remaining unchanged if we change t to $-t$. The reciprocity means the system is reciprocal, i.e. if for input a and b, the system output is c and d, then if we give input c and d to the system, it will give a and b as output. These conditions impose some constraints on the parameters involved in the system. Zhao *et al* described the TCMT formalism for all these cases separately, where a system satisfied only one of the three properties [33].

In recent years, the TCMT has been used to analyze the coupling of many devices. Wang described the TCMT formalism for nonreciprocal coupled systems, e.g. optical circulators [29]. Haus and Huang used a variational approach to derive the coupled equations for passive electromagnetic devices in time [14]. The basic idea is to write the trial solution as a linear combination of the normal modes of the uncoupled system. The expressions for the coupling coefficients are also given through this approach. Fan *et al* used TCMT formalism to describe the Fano resonance in optical resonators [9]. A single-mode optical resonator coupled with $m-$ports is considered in this case. One can also use TCMT formalism for wireless power transfer between two optical resonators [25]. A general TCMT formalism for describing the coupling between two resonators can be found here [30].

Photonic crystals are widely used for the processing of optical information. Directly coupled resonators, side-coupled resonators, and Fano-interference configurations are examples of such devices. One can use TCMT formalism to understand the coupling between such devices [2, 5, 7, 8, 16].

Timofeev *et al* used the TCMT formalism to describe the spectral behavior of Chiral Optical Tamm States that are especially localized states, formed at the interference of a mirror and chiral medium [28].

A plasmon is a group of oscillations of conductive electrons at the surface of metals, and an exciton is an electron and electron–hole pair in molecules or semiconductors. The coupling between the plasmon and the exciton is a plexciton system. The study of scattering, absorption, and luminescence spectra of the plexciton system is carried out by TCMT formalism for weak and strong coupling [15]. The system is considered lossy, and the losses are described by the parameters $\gamma_{\mathrm{pr}}, \gamma_{\mathrm{or}}$ (radioactive decay) and $\gamma_{\mathrm{pn}}, \gamma_{\mathrm{on}}$ (non-radioactive decay). Adato *et al* by motivating from the coupled damped harmonic oscillator (i.e. two mass-spring systems connected), the coupling between a plasmonic resonance and a weak molecular resonance is described using TCMT [1].

The TCMT technique was unsuccessful in dealing with coupled systems that had resonances with low-quality factors. Zhang and Miller developed a quasinormal CMT (QCMT), which is a framework similar to CMT but specifically designed for systems with significant losses [17, 32]. They compared TCMT and QCMT and found that QCMT exhibited remarkably accurate results. The quasinormal modes are the eigenfunctions for the non-Hermitian operators. Further development for QCMT can be found in [4, 27].

The CMT approach can also be used to describe the interactions between two non-linear coupled systems [20, 21]. The fundamental principle of the TCMT and its development for both linear and nonlinear coupled systems over the years is discussed in [6]. In this paper, we restrict ourselves to linear coupled problems.

In section 2, we discuss Haus's approach to decoupling individual LC circuit equations. A complicated Hamiltonian can be changed into a simpler Hamiltonian by using the canonical transformation without changing the physical properties of the system. We derive the same equations by defining canonical transformations and using them in the 'Hamiltonian' of the LC circuit. In section 3, we use the same approach for coupled LC circuits and develop an exact 4×4 system. The 4×4 system is shrunk even further to get a 2×2 system that is similar to equation (2) but has correction terms in the natural frequencies ω_1, ω_2. We also obtained

the exact expression for the parameters κ_{12}, κ_{21}. In the subsequent section 4, a numerical comparison is conducted among three models: the exact 4×4 model, the reduced 4×4 model, and the Haus model, where one can see the errors in the Haus model. Further, a mathematical analysis is carried out to identify the effect of approximations, revealing that the Haus model is a mathematical representation that provides a first-order approximation of the interaction between two systems.

2. Background

Haus presented how two general systems can be coupled using an LC circuit as an example and came up with the phenomenological equation [13]. This paper also considers two LC circuits coupled through a series coupling capacitor C_c that can be generalized to describe the coupling between any two systems in the time domain. An LC circuit model is chosen because it allows for easy handling of analytical expressions. For electric circuits, i is used to represent the current in the circuit; therefore, the square root of -1 is represented by j.

2.1. Uncoupled LC circuit model

For the uncoupled LC circuit, using Kirchoff's law, the relationship between the voltage v and the current i is given by

$$\frac{\mathrm{d}}{\mathrm{d}t}\begin{bmatrix} i \\ v \end{bmatrix} = \begin{bmatrix} 0 & -\frac{1}{L} \\ \frac{1}{C} & 0 \end{bmatrix}\begin{bmatrix} i \\ v \end{bmatrix}, \tag{3}$$

where L is the inductance and C is the capacitance. Note that the current direction considered here is opposite to that used by Haus. While this does not affect the LC circuit's physical interpretation or mathematical properties, it will cause a sign change in certain places, such as a negative sign in the expression for the coupling constant in equation (13).

The matrix $\begin{bmatrix} 0 & -\frac{1}{L} \\ \frac{1}{C} & 0 \end{bmatrix}$ has eigenvalues $\lambda_{\pm} = \pm j\omega_0$ where $\omega_0 = \frac{1}{\sqrt{LC}}$ is known as the natural frequency of oscillations. The matrix A is diagonalizable over $\mathbb{C}$. Using the eigenvectors to define functions

$$a^{\pm} = \sqrt{\frac{C}{2}}\left(v \mp j\sqrt{\frac{L}{C}}i\right), \tag{4}$$

where $\sqrt{\frac{C}{2}}$ is the normalization factor. The functions $a^{\pm}$ corresponding to the eigenvalues $\lambda_{\pm}$ represent the wave propagating in the positive and negative direction, respectively. Also note that in the case of the Haus model, we have the following relationship between the two modes of oscillation:

$$a^{-} = \left(a^{+}\right)^{*}. \tag{5}$$

Using these functions, one can decouple the system (3) and gets [13]

$$\begin{aligned} \frac{\mathrm{d}a^{+}}{\mathrm{d}t} &= j\omega_0 a^{+}, \\ \frac{\mathrm{d}a^{-}}{\mathrm{d}t} &= -j\omega_0 a^{-}. \end{aligned} \tag{6}$$

Equation (6) can be easily solved, and using (4), one can get the desired $v(t)$ and $i(t)$. Moreover, as a^- is conjugate to a^+, one can solve only the equation for a^+ and then, by using the relation (5), find a^-. This reduces the dimension of the problem. Next, we see how a similar approach can be extended to study the coupling between two systems.

2.2. Phenomenological model of coupled LC circuit by Haus

Consider two LC circuits connected through a series coupling capacitor C_c as shown in figure 2.

Haus gave a phenomenological model to explain the time-dependent coupling between the two LC circuits. Haus assumed the negative frequency component $a^-_{1,2}$ in the coupled system did not affect the positive frequency components $a^+_{1,2}$ and vice-versa. In literature, this is known as co-directional coupling [13]. Thus, by considering only the positive frequency component of the individual LC circuits, the interaction between a_1^+ and a_2^+ is modeled as:

$$\frac{\mathrm{d}}{\mathrm{d}t}\begin{bmatrix} a_1^+ \\ a_2^+ \end{bmatrix} = \begin{bmatrix} j\omega_1 & \kappa_{1+2+} \\ \kappa_{2+1+} & j\omega_2 \end{bmatrix}\begin{bmatrix} a_1^+ \\ a_2^+ \end{bmatrix}. \tag{7}$$

For the given system (7), there are four parameters: $\omega_1, \omega_2, \kappa_{1+2+}$ and κ_{2+1+}. Two of these four parameters ω_1 and ω_2 (angular frequencies) are known: $\omega_1 = \frac{1}{\sqrt{L_1C_1}}$ and $\omega_1 = \frac{1}{\sqrt{L_2C_2}}$. The other two parameters, which represent the coupling coefficients, κ_{1+2+} and κ_{2+1+}, are unknown at this moment. Here κ_{1+2+} is a measure of effect of coupling of the mode a_2^+ on the mode a_1^+.

In [13], Haus gave the expression for the total energy of the system (7) as

$$E = |a_1^+|^2 + |a_2^+|^2. \tag{8}$$

The conservation of the energy gives the condition on the parameters $\kappa_{1+2+}, \kappa_{2+1+}$. Consider

$$\begin{aligned}\frac{\mathrm{d}}{\mathrm{d}t}\left(|a_1^+|^2 + |a_2^+|^2\right) &= a_1^+\frac{\mathrm{d}a_1^{+*}}{\mathrm{d}t} + a_1^{+*}\frac{\mathrm{d}a_1^+}{\mathrm{d}t} + a_2^+\frac{\mathrm{d}a_2^{+*}}{\mathrm{d}t} + a_2^{+*}\frac{\mathrm{d}a_2^+}{\mathrm{d}t}, \quad \text{(Using (7))} \\ &= \left(\kappa_{1+2+} + \kappa^*_{2+1+}\right)a_1^{+*}a_2^+ + \left(\kappa^*_{1+2+} + \kappa_{2+1+}\right)a_1^+a_2^{+*}.\end{aligned}$$

The quantity $\frac{\mathrm{d}}{\mathrm{d}t}\left(|a_1^+|^2 + |a_2^+|^2\right) = 0$ if

$$\kappa_{1+2+} = -\kappa^*_{2+1+}. \tag{9}$$

This condition on the parameters makes the system matrix in equation (7) skew-Hermitian. The eigenvalues of the skew-Hermitian matrix are purely imaginary, which implies the existence of a closed orbit in the system. The physical interpretation of the closed orbit in a system implies the conservation of energy [26]. Thus, mathematically, the skew-Hermitian system matrix in equation (7) gives the conservation of energy.

If we consider the complete 4×4 model of Haus, which also includes negative components, the governing equation is as follows:

$$\frac{\mathrm{d}a}{\mathrm{d}t} = Ma, \tag{10}$$

where

$$M = \begin{bmatrix} j\omega_1 & \kappa_{1+2+} & 0 & 0 \\ \kappa_{2+1+} & j\omega_2 & 0 & 0 \\ 0 & 0 & -j\omega_1 & \kappa^*_{1+2+} \\ 0 & 0 & \kappa^*_{2+1+} & -j\omega_2 \end{bmatrix} \tag{11}$$

and

$$a = \begin{bmatrix} a_1^+ & a_2^+ & a_1^- & a_2^- \end{bmatrix}^T. \tag{12}$$

2.2.1. Limitation of the Haus model. Haus [13] further gave the values of the parameters $\kappa_{1^+2^+}, \kappa_{2^+1^+}$ as

$$\kappa_{1^+2^+} = \frac{-jC_c}{2\sqrt{C_1C_2}}\omega_2, \qquad \kappa_{2^+1^+} = \frac{-jC_c}{2\sqrt{C_1C_2}}\omega_1. \tag{13}$$

As mentioned in section 2.1, these expressions include a negative sign due to the difference in the reference direction. However, the relation in equation (9) remains valid. Using these values of the parameters $\kappa_{1^+2^+}, \kappa_{2^+1^+}$ in equation (9), we get $\omega_1 = \omega_2$. This shows that the Haus model given by (7) or (10) works well only for the identical oscillators. What happens if the two oscillators are non-identical? We address this question in section 3.2. Haus also mentioned that the values of the parameters $\kappa_{1^+2^+}, \kappa_{2^+1^+}$ are approximate, and improved values are either the arithmetic or the geometric mean of the natural frequencies ω_1 and ω_2. In section 3.2, we derive the correct values of coupling coefficients.

2.2.2. Model of coupled pendulums based on the Haus model. Louisell used the equation (7) to describe the coupling between linear pendulums of mass m and lengths l_1, l_2 which are coupled through spring with a spring constant k [19]. By considering the power transfer from system 1 to system 2, the coupling coefficients $\kappa_{1^+2^+}, \kappa_{2^+1^+}$ are evaluated as

$$\kappa_{1^+2^+} = \frac{-jk}{2m\sqrt{\omega_1\omega_2}}, \qquad \kappa_{2^+1^+} = \frac{-jk}{2m\sqrt{\omega_1\omega_2}}. \tag{14}$$

The expressions in equation (14) are based upon two assumptions: One is the average over each cycle of oscillation for pendulum 1; i.e. the term kx_1v_1 is neglected in the derivation as x_1 and v_1 are correlated such that kx_1v_1 had a negligible effect on the power transferred to the pendulum 1, and also, the above expressions are true only if $\omega_1^2 \cong \omega_2^2$. In the next section, we derive the CMT Equations and find the values of parameters $\kappa_{1^+2^+}$ and $\kappa_{2^+1^+}$ without using any approximations, as elaborated further.

3. Hamiltonian approach for LC circuit models

3.1. Hamiltonian approach for uncoupled LC circuit model

The Hamiltonian of a system is the sum of kinetic energy and potential energy. The Hamiltonian can also be found from the Lagrangian by using the Legendre transformation. The Lagrangian for a system is given by the difference between kinetic and potential energy. The 'kinetic energy' of the LC circuit is $\frac{1}{2}L\dot{q}^2$ [23]. The energy stored in the capacitor can be interpreted as the potential energy for the LC circuit. Thus, the 'potential energy' of the LC circuit is $\frac{1}{2}\frac{q^2}{C}$, where q is the charge in the circuit, $v = \frac{q}{C}$, and $i = \frac{\mathrm{d}q}{\mathrm{d}t}$.

Thus, the Lagrangian of the LC circuit system is given by

$$\pounds(q,\dot{q}) = \frac{1}{2}L\dot{q}^2 - \frac{1}{2}\frac{q^2}{C}. \tag{15}$$

'The equation of motion' for the LC circuit can be found by using the Euler–Lagrange equation

$$\frac{\mathrm{d}}{\mathrm{d}t}\left(\frac{\partial \pounds}{\partial \dot{q}}\right) - \frac{\partial \pounds}{\partial q} = 0 \tag{16}$$

for the Lagrangian (15), which will give a second-order differential equation

$$\ddot{q} + \omega_0^2 q = 0, \tag{17}$$

where $\omega_0 = \frac{1}{\sqrt{LC}}$.

To find the Hamiltonian from the Lagrangian, one needs to define generalized coordinates $P = \frac{\partial \pounds}{\partial \dot{q}} = L\dot{q}$ and $Q = q$.

One can find the Hamiltonian from the above Lagrangian in equation (15) using the Legendre transformation as [12]

$$H(P,Q) = P\dot{q} - \pounds(q,\dot{q}) = \frac{1}{2}\frac{P^2}{L} + \frac{1}{2}\frac{Q^2}{C}, \tag{18}$$

where $P = \frac{\partial \pounds}{\partial \dot{q}}$ and $Q = q$ are generalized coordinates for current and charge, respectively.

Hamilton's equations of motion are given by

$$\begin{aligned} \dot{Q} &= \frac{\partial H}{\partial P} = \frac{P}{L}, \\ \dot{P} &= -\frac{\partial H}{\partial Q} = -\frac{Q}{C}. \end{aligned} \tag{19}$$

From equation (19), one can get equation (17). Thus, both the approaches in equations (16) and (18) give the same results.

One of the advantages of using the Hamiltonian over the Lagrangian is that it allows the change of coordinates through canonical transformation. A canonical transformation preserves Hamilton's equation of motion [12]. The objective of using canonical transformations in the Hamiltonian is to reduce the complexity of Hamilton's equations of motion.

In the case of the LC circuit, we decouple the system in equation (3) by defining appropriate canonical transformation. As we know, the eigenvectors are unique up to multiplicative constant; the canonical transformations defined further are also motivated by the eigenvectors.

Now we derive the decouple equations for the LC circuit in figure 1 using canonical transformations [12]. Let f and g be functions of coordinates Q, P. Then f and g are canonical if

$$\{f,g\} = \frac{\partial f}{\partial Q}\frac{\partial g}{\partial P} - \frac{\partial g}{\partial Q}\frac{\partial f}{\partial P} = 1$$

or we can say their Jacobian

$$J = \begin{vmatrix} \frac{\partial f}{\partial Q} & \frac{\partial f}{\partial P} \\ \frac{\partial g}{\partial Q} & \frac{\partial g}{\partial P} \end{vmatrix} = 1.$$

The brackets $\{f,g\}$ are called the Poisson brackets. Our next objective is to define the canonical transformations, through which we obtain a new Hamiltonian for the LC circuit whose equations of motion are decoupled.

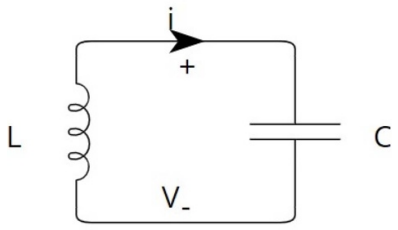

Figure 1. LC circuit: capacitor C and inductor L are connected in parallel.

We construct the following transformations using the functions related to the eigenvectors of the system of first-order differential equation (3) and using the condition $\{a^+, a^-\} = 1$:

$$a^{\pm} = \mp\sqrt{j}(LC)^{\frac{1}{4}}\sqrt{\frac{L}{2}}\left(\frac{P}{L} \pm j\frac{1}{\sqrt{LC}}Q\right). \tag{20}$$

Note that the amplitudes a^+ and a^- are related to each other. One can see this by expanding the term $\sqrt{j}$ and taking the complex conjugate of a^+, we get

$$a^- = \exp\left(-j\frac{\pi}{2}\right)\left(a^+\right)^*. \tag{21}$$

Here, a^+ represents a wave going in the anti-clockwise direction, and a^- represents a wave in the direction of $(a^+)^*$ with a phase lag of $\frac{\pi}{2}$. Thus, if we know a^+, we can find a^- by using the above relation. Comparing this expression with that of in equation (5) shows that here we have an additional phase factor. As we will see later in section 4, the presence of phase factor improves the accuracy of the reduced order model obtained with the canonical transformation-based Hamiltonian approach.

From equation (20), we have

$$P = -\sqrt{\frac{L}{2j}}\left(\frac{1}{LC}\right)^{\frac{1}{4}}\left(a^+ - a^-\right), \tag{22}$$

$$Q = j\sqrt{\frac{C}{2j}}\left(\frac{1}{LC}\right)^{\frac{1}{4}}\left(a^+ + a^-\right). \tag{23}$$

From equation (18), the Hamiltonian for the uncoupled LC-circuit becomes

$$H\left(a^+, a^-\right) = \frac{\omega_0}{4j}\left[\left(a^+ - a^-\right)^2 - \left(a^+ + a^-\right)^2\right] = j\omega_0 a^+ a^-. \tag{24}$$

The following equations give the dynamics for the above Hamiltonian [12]

$$\dot{a}^+ = \frac{\partial H}{\partial a^-},$$
$$\dot{a}^- = -\frac{\partial H}{\partial a^+}.$$

Thus, we have

$$\dot{a}^+ = j\omega_0 a^+, \tag{25}$$

$$\dot{a}^- = -j\omega_0 a^-. \tag{26}$$

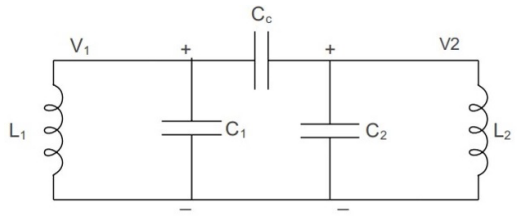

Figure 2. Coupled LC-circuit: two LC-circuits with capacitor C_1, C_2 and inductor L_1, L_2 are connected in series with a coupling capacitor C_c.

Note that the form of these equations is the same as that of earlier derived equations in equation (6), but the transformation functions $a^{\pm}$ are different.

Since there are no losses in the circuit, the Hamiltonian $H(a^+, a^-)$ in equation (24) must be conserved. As shown by the following calculations, it is indeed true:

$$\frac{\mathrm{d}H}{\mathrm{d}t} = \frac{\omega_0}{4j}\left[2\left(a^+ - a^-\right)\left(\dot{a}^+ - \dot{a}^-\right) - 2\left(a^+ + a^-\right)\left(\dot{a}^+ + \dot{a}^-\right)\right] = 0.$$

In this section, the decoupling of the LC circuit system is achieved by using the canonical transformations in the Hamiltonian. These canonical transformations are obtained with the help of the functions related to the eigenvectors of the system. We use a similar approach to analyze the coupled LC circuit system in the subsequent part.

3.2. Hamiltonian approach for coupled LC circuit model

Now we define the Hamiltonian for the coupled LC circuit and, using the similar canonical transformation (20), we derive a 4×4 system of first-order differential equations with exact values of the parameters $\kappa_{1^+2^+}, \kappa_{2^+1^+}$.
For coupled LC circuit in figure 2, the Hamiltonian is [23]

$$H = \frac{1}{2}\frac{P_1^2}{L_1} + \frac{1}{2}\frac{P_2^2}{L_2} + \frac{1}{2}\frac{Q_1^2}{C_1} + \frac{1}{2}\frac{Q_2^2}{C_2} + \frac{1}{2}C_c\left(\frac{Q_1}{C_1} - \frac{Q_2}{C_2}\right)^2, \tag{27}$$

where C_c is the coupling capacitor and Q_1, P_1, Q_2, P_2 are the generalized coordinates for the charges and generalized currents of the circuit 1 and 2, respectively.
Again, motivating from equation (20), consider the transformations,

$$\begin{aligned} a_1^{\pm} &= \mp\sqrt{j}\,(L_1C_1)^{\frac{1}{4}}\sqrt{\frac{L_1}{2}}\left(\frac{P_1}{L_1} \pm j\frac{1}{\sqrt{L_1C_1}}Q_1\right), \\ a_2^{\pm} &= \mp\sqrt{j}\,(L_2C_2)^{\frac{1}{4}}\sqrt{\frac{L_2}{2}}\left(\frac{P_2}{L_2} \pm j\frac{1}{\sqrt{L_2C_2}}Q_2\right). \end{aligned} \tag{28}$$

Similar to (21), here we have the following relationship between positive and negative frequency components:

$$a_{1,2}^- = \exp\left(\frac{-j\pi}{2}\right)\left(a_{1,2}^+\right)^*. \tag{29}$$

One can check that the above transformations are canonical as $\{a_1^+, a_1^-\} = 1, \{a_1^+, a_2^+\} = \{a_1^+, a_2^-\} = \{a_1^-, a_2^+\} = \{a_1^-, a_2^-\} = 0, \{a_2^+, a_2^-\} = 1$. From the above transformations (28), we have

$$
\begin{aligned}
P_1 &= -\sqrt{\frac{L_1}{2j}}\left(\frac{1}{L_1C_1}\right)^{\frac{1}{4}}\left(a_1^+ - a_1^-\right),\\
Q_1 &= j\sqrt{\frac{C_1}{2j}}\left(\frac{1}{L_1C_1}\right)^{\frac{1}{4}}\left(a_1^+ + a_1^-\right),\\
P_2 &= -\sqrt{\frac{L_2}{2j}}\left(\frac{1}{L_2C_2}\right)^{\frac{1}{4}}\left(a_2^+ - a_2^-\right),\\
Q_2 &= j\sqrt{\frac{C_2}{2j}}\left(\frac{1}{L_2C_2}\right)^{\frac{1}{4}}\left(a_2^+ + a_2^-\right).
\end{aligned}
$$

Using these values in the Hamiltonian for the coupled LC-circuit, equation (27) becomes

$$
\begin{aligned}
H\left(a_1^{\pm}, a_2^{\pm}\right) = \frac{\omega_1}{4j}\left[\left(a_1^+ - a_1^-\right)^2 - \left(a_1^+ + a_1^-\right)^2\right] + \frac{\omega_2}{4j}\left[\left(a_2^+ - a_2^-\right)^2 - \left(a_2^+ + a_2^-\right)^2\right]\\
+ \frac{C_c}{4j}\left[-\frac{\omega_2}{C_2}\left(a_2^+ + a_2^-\right)^2 - \frac{\omega_1}{C_1}\left(a_1^+ + a_1^-\right)^2 + 2\left(a_2^+ + a_2^-\right)\left(a_1^+ + a_1^-\right)\frac{\sqrt{\omega_1\omega_2}}{\sqrt{C_1C_2}}\right].
\end{aligned}
\tag{30}
$$

From equation (30), the following equations give the dynamics of the coupled LC circuits

$$
\begin{aligned}
\dot{a_1}^+ &= \frac{\partial H}{\partial a_1^-},\\
\dot{a_1}^- &= -\frac{\partial H}{\partial a_1^+},\\
\dot{a_2}^+ &= \frac{\partial H}{\partial a_2^-},\\
\dot{a_2}^- &= -\frac{\partial H}{\partial a_2^+}.
\end{aligned}
\tag{31}
$$

The system of equations in matrix form

$$
\frac{\mathrm{d}a}{\mathrm{d}t} = Aa, \tag{32}
$$

where

$$
A = \begin{bmatrix}
j\left(\omega_1 + \frac{C_c\omega_1}{2C_1}\right) & \kappa_{1+2+} & \frac{jC_c\omega_1}{2C_1} & \kappa_{1+2-}\\
\kappa_{2+1+} & j\left(\omega_2 + \frac{C_c\omega_2}{2C_2}\right) & \kappa_{2+1-} & \frac{jC_c\omega_2}{2C_2}\\
-\frac{jC_c\omega_1}{2C_1} & \kappa_{1-2+} & -j\left(\omega_1 + \frac{C_c\omega_1}{2C_1}\right) & \kappa_{1-2-}\\
\kappa_{2-1+} & -\frac{jC_c\omega_2}{2C_2} & \kappa_{2-1-} & -j\left(\omega_2 + \frac{C_c\omega_2}{2C_2}\right)
\end{bmatrix}
\tag{33}
$$

and a is as in equation (12), and

$$\begin{aligned}\kappa_{1^+2^+} = \kappa_{1^+2^-} = \kappa_{2^+1^+} = \kappa_{2^+1^-} &= -j\frac{C_c}{2\sqrt{C_1C_2}}\sqrt{\omega_1\omega_2},\\ \kappa_{1^-2^+} = \kappa_{1^-2^-} = \kappa_{2^-1^+} = \kappa_{2^-1^-} &= j\frac{C_c}{2\sqrt{C_1C_2}}\sqrt{\omega_1\omega_2}.\end{aligned} \tag{34}$$

Equation (32) represents the exact 4×4 system that explains the dynamics of the coupled LC circuits. Earlier in the Haus model (7), the amplitudes a_1^+, a_2^+ were evolving with natural frequencies ω_1, ω_2 respectively. The quantities $\frac{C_c\omega_1}{2C_1}$, $\frac{C_c\omega_2}{2C_2}$ are the corrections in the natural frequencies ω_1, ω_2 respectively. These corrections can also be interpreted as self-coupling terms.

From equation (32), we can see a_1^- and a_2^- are also affecting the dynamics of a_1^+, whereas earlier in the Haus model (7), the dynamics of a_1^+ is effected by a_2^+ only; i.e. the effect of a_1^-, a_2^- was neglected (co-directional coupling).

The parameters $\kappa_{1^+2^+}$ and $\kappa_{1^+2^-}$ represent the effect of coupling on a_1^+ from a_2^+ and a_2^-, and the parameters $\kappa_{2^+1^+}$ and $\kappa_{2^+1^-}$ represent the effects of coupling on a_2^+ from a_1^+ and a_1^-. The values for κ's in equation (34) are the exact expressions. As predicted by Haus, the values of the parameters are the geometric mean of the natural frequencies ω_1, ω_2 with the same constants $\frac{-jC_c}{2\sqrt{C_1C_2}}$ as in equation (13). The energy conservation for the Haus model gives the condition on the parameter $\kappa_{12} = -\kappa_{21}^*$ which further gives $\omega_1 = \omega_2$. The Hamiltonian given in equation (30) is the conserved quantity for the 4×4 exact system, which does not put any restriction on the parameters involved in the system and on the oscillation frequencies ω_1, ω_2. If we assume $\omega_1 = \omega_2 = \omega$ in the exact system, we get $\kappa_{1^+2^+} = \frac{-jC_c}{2\sqrt{C_1C_2}}\omega$ which is the same as approximated by Haus in equation (13).

Thus far, we have derived the uncoupled equations for the LC circuit and the 4×4 system for the coupled LC circuits by the Hamiltonian approach. We also see the relationship between a_1^+, a_1^-. By motivating from the above relationship between a_1^+, a_1^-, we reduce the system in equation (32) to a 2×2 system in the next part. The reduced system is like the Haus model, with some modifications, and gives exact expressions for coupling coefficients κ-s. Later in section 4, we show that this reduced model is more accurate than the Haus model.

3.2.1. Reduced model. The system (32) can be further simplified by assuming the coupling is effective only for the co-directional normal modes, e.g. in the present case of the coupled LC circuits; it means considering the coupling only between the positive frequency component. That amounts to neglecting the effect of negative components a_1^-, a_2^- from the differential equation of positive components a_1^+, a_2^+. This reduced system is given as:

$$\frac{\mathrm{d}a}{\mathrm{d}t} = Ra, \tag{35}$$

where

$$R = \begin{bmatrix} j\left(\omega_1 + \frac{C_c\omega_1}{2C_1}\right) & \kappa_{1^+2^+} & 0 & 0\\ \kappa_{2^+1^+} & j\left(\omega_2 + \frac{C_c\omega_2}{2C_2}\right) & 0 & 0\\ 0 & 0 & -j\left(\omega_1 + \frac{C_c\omega_1}{2C_1}\right) & \kappa_{1^-2^-}\\ 0 & 0 & \kappa_{2^-1^-} & -j\left(\omega_2 + \frac{C_c\omega_2}{2C_2}\right) \end{bmatrix}$$

and $a = \begin{bmatrix} a_1^+ & a_2^+ & a_1^- & a_2^- \end{bmatrix}^{\mathrm{T}}$. This reduced model is similar to the Haus model, but with a correction in the natural frequencies ω_1, ω_2 and the exact value of the coupling coefficients κ-s (34).

Using the relationship (29), one can also consider the 2×2 reduced model:

$$\begin{bmatrix} \dot{a}_1^+ \\ \dot{a}_2^+ \end{bmatrix} = \begin{bmatrix} j\left(\omega_1 + \frac{C_c\omega_1}{2C_1}\right) & \kappa_{1^+2^+} \\ \kappa_{2^+1^+} & j\left(\omega_2 + \frac{C_c\omega_2}{2C_2}\right) \end{bmatrix} \begin{bmatrix} a_1^+ \\ a_2^+ \end{bmatrix}. \tag{36}$$

In the approximated model (36), the system matrix involved is a Hermitian matrix. If we consider a resistor in the LC circuit in figure 2 (i.e. the set-up of a parallel RLC circuit), the system will exhibit losses. For such a system, the Lagrangian and Hamiltonian formulation is complicated. One can use the approach followed by Haus by replacing ω_0 by $\omega_0 + j\alpha_0$, where α_0 represents the losses in the system [13]. Similar modification can also be incorporated in the model (36). The relation (9) $\kappa_{1^+2^+} = -\kappa^*_{2^+1^+}$ will not hold, and the system matrix in equation (36) is non-Hermitian matrix.

3.2.2. Error analysis. Neglecting the negative components from the exact system (32) introduces errors in the Haus model and the reduced model. Let $\dot{X} = AX$ represents the exact system and $\dot{x} = Rx$ represents the reduced model. Then, the error E_R in the approximated model can be found by putting the exact solution X in $\dot{x} = Rx$. Thus

$$E_R = \dot{X} - RX = AX - RX = (A - R)X.$$

The norm of the matrix $(A - R)$ gives the bound for the error. Since the system (32) is finite-dimensional, all the norms are equivalent. The standard norm on the matrix is the Frobenius norm, which for any square matrix D of order n can be given

$$\|D\|_F = \left[\sum_{i=1}^{n}\sum_{j=1}^{n} |d_{i,j}|^2\right]^{\frac{1}{2}} = \sqrt{\mathrm{trace}\,(D^*D)}.$$

The error for the reduced model is

$$\begin{aligned} \|E_R\|_F^2 = \|A-R\|_F^2 &= \mathrm{trace}\left((A-R)^*(A-R)\right), \\ &= 2\left(\frac{C_c\omega_1}{C_1}\right)^2 + 2\left(\frac{C_c\omega_2}{C_2}\right)^2 + |\kappa_{1^-2^+}|^2 + |\kappa_{1^+2^-}|^2 + |\kappa_{2^+1^-}|^2 + |\kappa_{2^-1^+}|^2, \\ &= 2\frac{C_c^2}{4}\left[\frac{\omega_1^2}{C_1^2} + \frac{\omega_2^2}{C_2^2}\right] + 4\frac{C_c^2\omega_1\omega_2}{4C_1C_2}. \qquad \text{(Using (34))} \end{aligned}$$

$$\text{Thus, } \|A-R\|_F = \frac{1}{\sqrt{2}}\left[\frac{C_c}{C_1}\frac{1}{\sqrt{L_1C_1}} + \frac{C_c}{C_2}\frac{1}{\sqrt{L_2C_2}}\right]. \tag{37}$$

Equation (37) gives the error of approximation for the reduced model (35). Since the physical dimension of the error is equal to the dimension of the frequency, which further depends upon the time period, the error in equation (37) is in terms of the time period of oscillations for the coupled system. From the error, we can conclude the following:

1. The approximation error tends to 0 if $C_c \ll C_1, C_2$; which is the case of the weak coupling. Thus, the reduced model works well for weak coupling.
2. From equation (37), the error in the reduced model is a linear term in frequencies ω_1, ω_2. Hence, the approximated model is a first-order approximation to the exact 4×4 model (32).

3. When the value of the coupling capacitor C_c is significantly larger than the values of the individual circuit capacitors C_1 and C_2; i.e. $C_c \gg C_1, C_2$, the reduced model exhibits a significant error. This is because the right side of equation (37) continues to increase as the value of C_c increases. Physically, one can interpret it as the frequency of energy exchange between the two systems increases. This can be further clear from the numerical simulations in section 4.
4. If $\frac{C_c}{C_1}$ and $\frac{C_c}{C_2}$ are of order ϵ, then $\|A-R\|_F \leqslant \frac{\epsilon}{\sqrt{2}} \max\{\omega_1, \omega_2\}$.

One can also find the relative error for the reduced model compared to the exact model (32). The relative error of the reduced model is given by $\frac{\|A-R\|_E}{\|A\|_F}$, where

$$\begin{aligned}\|A\|_F^2 &= 2\left[\omega_1^2\left(1+\frac{C_c}{2C_1}\right)+\omega_2^2\left(1+\frac{C_c}{2C_2}\right)+\frac{C_c^2}{2}\left(\frac{\omega_1}{C_1}+\frac{\omega_2}{C_2}\right)^2\right] \\ &\geqslant 2\max\left\{\omega_1^2, \omega_2^2\right\}.\end{aligned}$$

Thus we have

$$\text{Relative error} = \frac{\|A-R\|_F}{\|A\|_F} \leqslant \epsilon \frac{\max\{\omega_1,\omega_2\}}{\max\{\omega_1,\omega_2\}} = \epsilon. \tag{38}$$

Thus, the relative error is of the order ϵ; i.e. $\mathcal{O}(\epsilon)$, if $\epsilon \to 0$, $E_r \to 0$; i.e. $C_c \ll C_1, C_2$, which implies weak coupling. Also, $\epsilon \gg 1$ implies the case of strong coupling.
The error for the Haus mode is

$$\|E_M\|_F^2 = \|A-M\|_F = \frac{C_c^2}{C_1^2}\omega_1^2 + \frac{C_c^2}{C_2^2}\omega_2^2 + 4|\kappa_{12}|^2 = 3\frac{C_c^2}{C^2}\frac{1}{LC}. \tag{39}$$

Error for the reduced model for identical LC circuits

$$\|A-R\|_F^2 = 2\frac{C_c^2}{C^2}\frac{1}{LC}. \tag{40}$$

From equations (39) and (40), we can conclude

$$\|A-R\|_F^2 = 2\frac{C_c^2}{C^2}\frac{1}{LC} < 3\frac{C_c^2}{C^2}\frac{1}{LC} = \|A-M\|_F^2. \tag{41}$$

The above equation shows the Haus model and the reduced model are first-order approximated models for the coupled LC circuits. Furthermore, the reduced model exhibits a higher accuracy than the Haus model.

In the next section, we numerically compare the performance of the three models: the exact model, the Haus model, and the reduced model for two LC circuits coupled with a series coupling capacitor as in figure 2. Simulations clearly show that the correction terms in the matrix of the reduced model (35) results in improved accuracy of the amplitude and phase of the wave, compared to the Haus model.

4. Numerical simulations

This section compares the three models: the exact 4×4 model, the Haus 4×4 model, and the reduced 4×4 model. As discussed in the section 2.2 (after equation (13)), the Haus model requires $\kappa_{1^+2^+} = -\kappa^*_{2^+1^+}$, leading to the constraint $\omega_1 = \omega_2$, first we will consider the case with two identical LC circuits coupled with each other.

4.1. Coupling of identical oscillators

Here we have $L_1 = L_2 = 6.8\ \mu$H and $C_1 = C_2 = 22\ \mu$F. We consider various cases where the value of the coupling capacitor C_c increases relative to the value of the capacitor C. Define the parameter $\epsilon = \frac{C_c}{C}$. When the value of ϵ equals zero, it indicates that two circuits are uncoupled. When the value of ϵ equals 1 gives $C_c = C$. The numerical solver used for this study is ODE45 with a relative tolerance of 10^{-6}.

Initially, we give voltage $v_1(0) = 1, i_1(0) = 0$ for the first circuit and $v_2(0) = 0; i_2(0) = 0$ for the second circuit in figure 2. Putting these initial values of voltages and currents in $a_1^{\pm}$ and $a_2^{\pm}$ gives the initial conditions for the exact model (32), the reduced model (35) and the Haus model (10).

For the Haus model, the initial conditions are:

$$\begin{aligned} a_1^{\pm}(0) &= \sqrt{\frac{C}{2}}\left(v_1(0) \mp j\sqrt{\frac{L}{C}} i_1(0)\right), \\ a_2^{\pm}(0) &= \sqrt{\frac{C}{2}}\left(v_2(0) \mp j\sqrt{\frac{L}{C}} i_2(0)\right). \end{aligned} \tag{42}$$

The voltage and current are related to the charge $v = \dfrac{Q}{C}$ and $i = \dot{Q}$, thus the initial voltage $v(0)$ gives $Q(0) = Cv(0)$ and $i(0) = \dot{Q}(0)$, where C is the capacitor of the circuit.

The initial conditions for the exact and the reduced model are as:

$$\begin{aligned} a_1^{\pm}(0) &= \mp\sqrt{j}(LC)^{\frac{1}{4}}\sqrt{\frac{L}{2}}\left(\dot{Q}_1(0) \pm \frac{j}{\sqrt{LC}} Q_1(0)\right), \\ a_2^{\pm}(0) &= \mp\sqrt{j}(LC)^{\frac{1}{4}}\sqrt{\frac{L}{2}}\left(\dot{Q}_2(0) \pm \frac{j}{\sqrt{LC}} Q_2(0)\right). \end{aligned} \tag{43}$$

4.1.1. Case 1: two systems are uncoupled. In this case, we consider both the identical systems uncoupled by taking the value of the coupling capacitor $C_c = 0\ \mu$F. The relationship between the currents and voltages of circuit 1 and 2 with respect to time are shown in figure 3. Since the two circuits are not connected, the current and voltage in the second circuit are always zero, as seen in figures 3(c) and (d). The three models provide the same results for the uncoupled system.

In the subsequent cases, we compare solutions of three models for different coupling capacitor C_c values and determine the maximum amount of weak coupling that permits almost exact solutions.

4.1.2. Case 2: two systems are weakly coupled. In this case, two identical LC circuits are weakly coupled, i.e. $0 < C_c \ll C_1 = C_2$. The value of the coupling capacitor $C_c = 0.22\ \mu$F which is 1 percent of the value of the capacitor $C = 22\ \mu$F; i.e. $\epsilon = 0.01$. The dynamics of the coupled system can be seen in figure 4.

Initially, $v_1(0) = 1, i_1(0) = 0$ and $v_2(0) = 2, i_2(0) = 0$, which are plotted as a point in figure 4. Since the two circuits are coupled, the voltage and current in the circuit 1 start decreasing, and the voltage and current in the circuit 2 start increasing. The relationship of voltages and currents of the circuits 1 and 2 with respect to time can be seen in figures 4(a)–(d). From figure 4, we can see all three models behave quite similar in this case. Figure 4(e) shows the energy transfer between circuit 1 and 2.

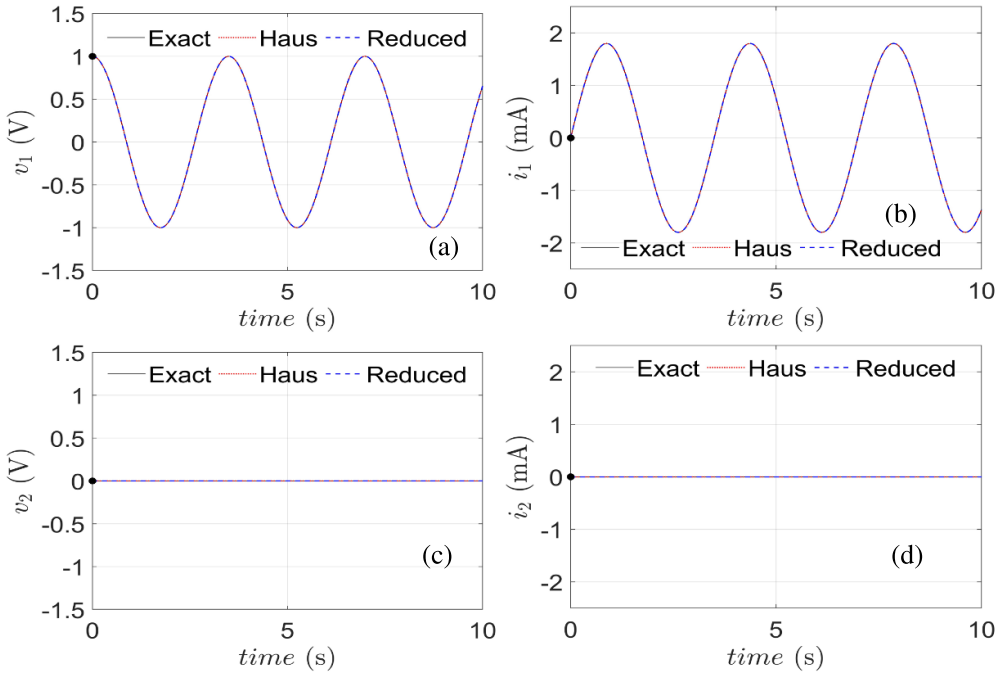

Figure 3. Case 1: figures (a)–(d) show the relationship between voltages and currents of the circuits 1 and 2 with respect to time. The coupling capacitor value is $C_c = 0$ μF.

4.1.3. Energy in the reduced model. In the Haus model set-up (4), the energy in the oscillator is given by $H = |a^+|^2$, whereas in the Hamiltonian model set-up (20), the energy in the oscillator is given by $H = \omega_0|a^+|^2$. Therefore, while describing the energy exchange in the reduced model for the coupled oscillators, the term $|a_1^+|^2$ is scaled by the corresponding angular frequency ω_1, such that $\omega_1|a_1^+|^2$ represents the energy in the circuit 1. Similarly, $\omega_2|a_2^+|^2$ represents the energy in the circuit 2. In the Haus model (7) of the coupled oscillators, $|a_1^+|^2$ and $|a_2^+|^2$ represent the energies in the circuit 1 and 2 respectively [13].

Figure 4(e), initially, the complete energy is in circuit 1; after some instants, the complete energy is transferred to the circuit 2, and there is no energy in the circuit 1 at that instant. Then, the process is reversed, and the complete energy gets back to the circuit 1. The period of exchange of energy between two circuits is called the coupling period h. The coupling period can be given by the equation [10]

$$h = \sqrt{\left(\frac{\Delta\omega}{2}\right)^2 + \kappa_{1^+2^+}\kappa_{2^+1^+}}, \tag{44}$$

where $\Delta\omega = \omega_1 - \omega_2$. In [10], the coupling period h was found for two coupled waveguides in the space domain. The same approach can be used here, which gives the coupling period as in equation (44). The coupling period h can also be seen in figure 4(e).

If we compare the Haus model (7) with the reduced model (36), the differences lie in the diagonal entries of the system matrix, (see the corrections for the natural frequencies ω_1 and ω_2), and the values of the coupling coefficients. In the case of identical oscillators, the coupling coefficients of the Haus model and the reduced model coincide, and the only differences are in

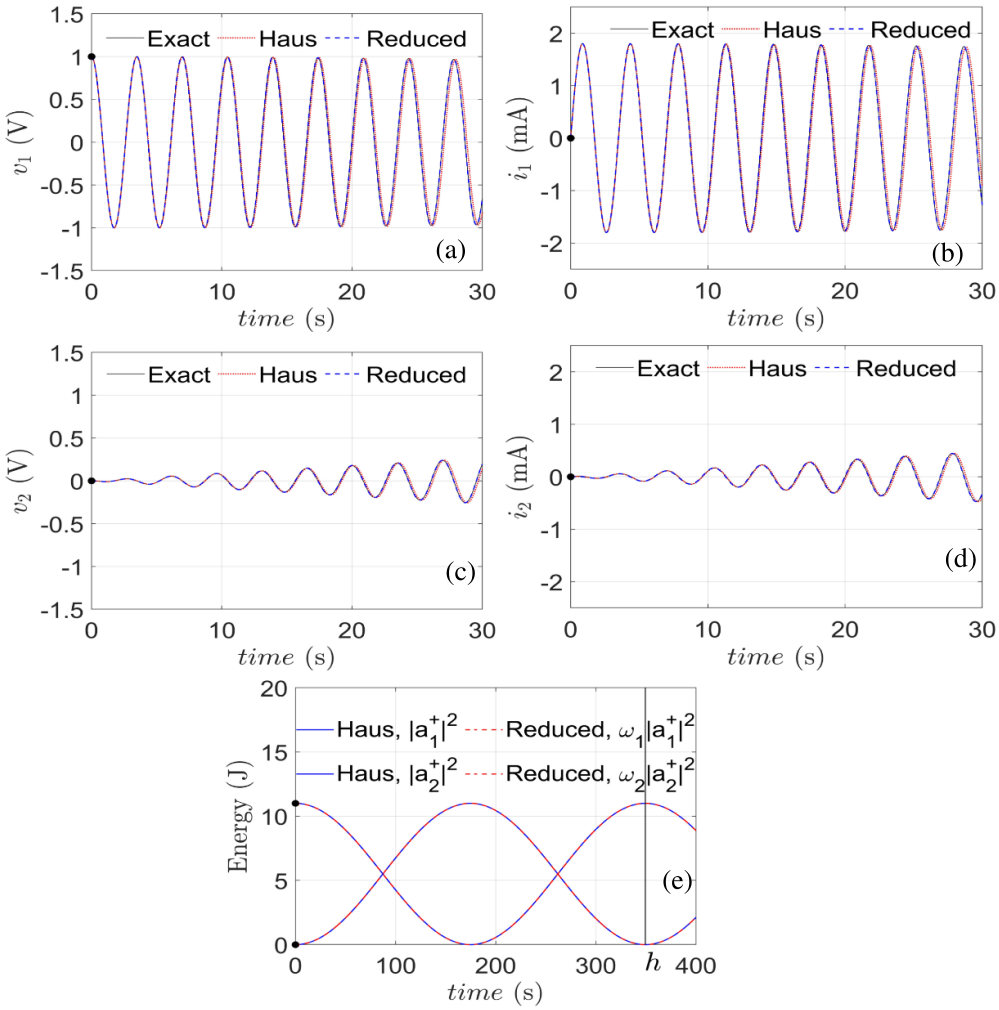

Figure 4. Case 2: figures (a)–(d) show the relationship between voltages and currents of the circuits 1 and 2 w.r.t. time. Figure (e) shows the energy exchange between the two circuits. The coupling capacitor value is $C_c = 0.22\ \mu$F.

the diagonal correction terms (which are purely imaginary quantities). This manifests as phase error, leaving the magnitude intact. Therefore, in the absence of any losses, both these models capture energy exchange exactly the same as shown in figure 4(e).

4.1.4. Case 3: not so weakly coupled. Here the value of the coupling capacitor $C_c = 2.2\ \mu$F, which is 10 percent of the value of the capacitor $C = 22\ \mu$F; i.e. $\epsilon = 0.1$. For this set-up, the relationship between the currents and voltages of the circuit 1 and 2 with respect to time is shown in figures 5(a)–(d). The results of the Haus model and the reduced model are quite similar at first, but after a few instants, the reduced model exhibits better approximation compared to the Haus model. The voltage and current in circuit 2 increases to a maximum and then decreases. The Haus model shows phase error and amplitude error, whereas the reduced

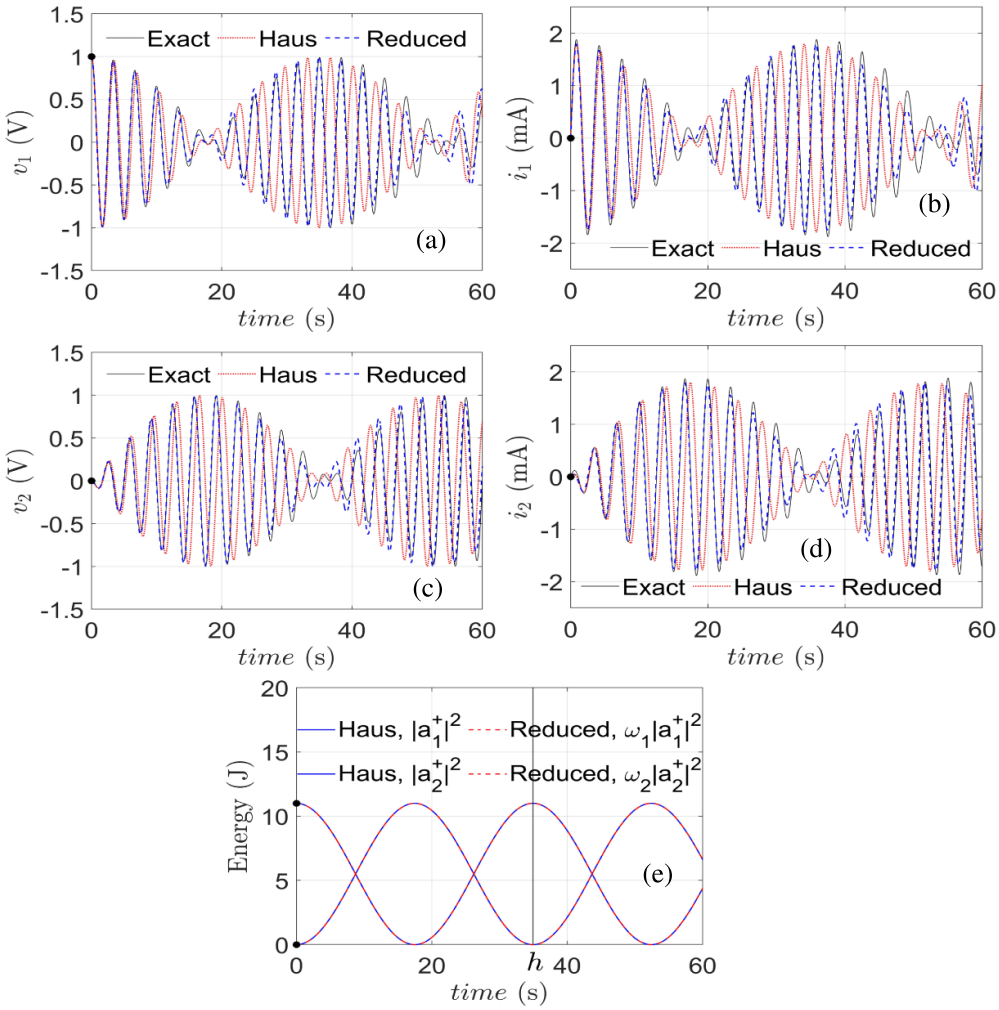

Figure 5. Case-3 figures (a)–(d) show the relationship between voltages and currents of the circuits 1 and 2 w.r.t. time. Figure (e) shows the energy exchange between two circuits. The coupling capacitor value is $C_c = 2.2\ \mu$F.

model shows accurate results. The energy exchange between the two circuits can be seen in figure 5(e).

4.1.5. Case 4: slightly strongly coupled. The value of the coupling capacitor $C_c = 5.5\ \mu$F, which is 25 percent of the value of the capacitor $C = 22\ \mu$F; i.e. $\epsilon = 0.25$.

For the value of the coupling capacitor $C_c = 5.5\ \mu$F, the relation between the currents and voltages with respect to time can be seen in figure 6. Due to the absence of the correction terms $\frac{C_c}{2C_1}\omega_1, \frac{C_c}{2C_2}\omega_2$ in the natural frequencies, the phase error in the Haus model shows a significant difference. Due to the presence of the correction terms, the reduced model shows fewer errors and gives more accurate results as compared to the Haus model. The phase and amplitude errors can also be seen in figures 6(a)–(d). Energy is exchanged between the two systems

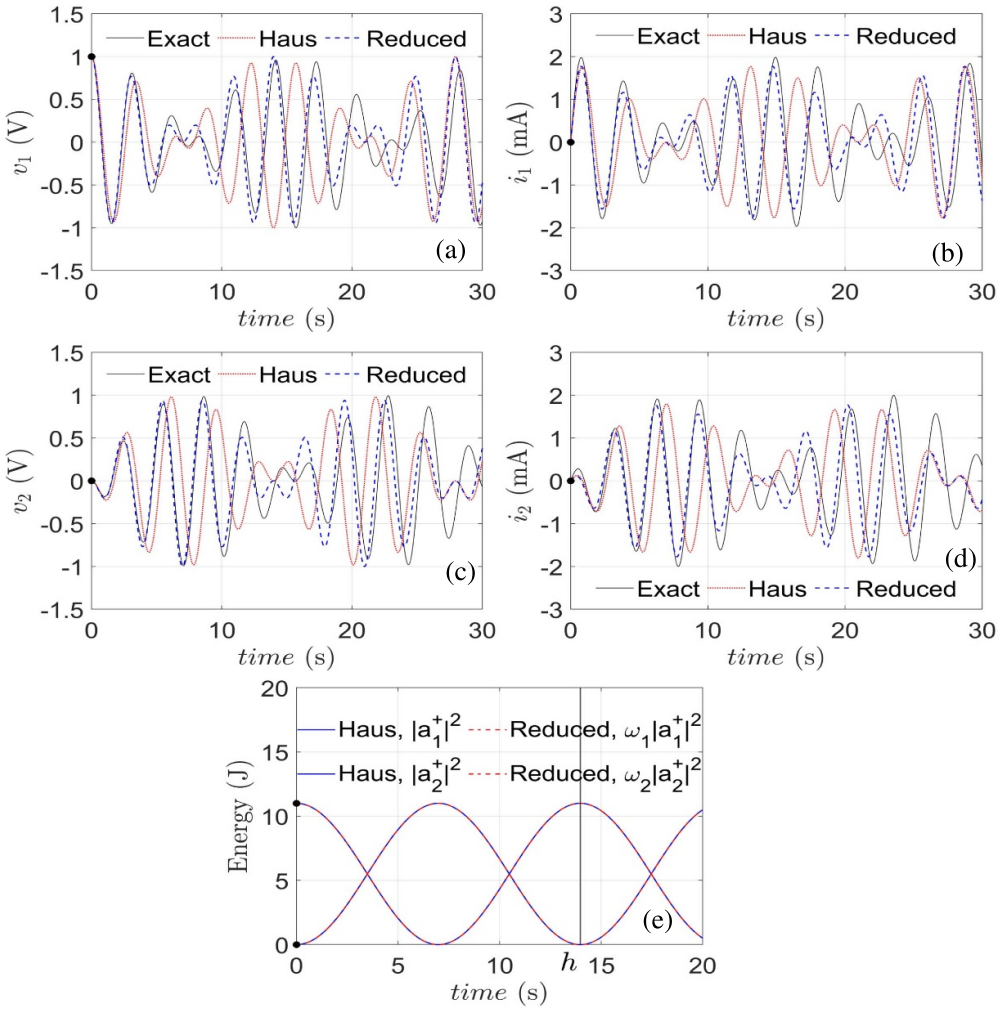

Figure 6. Case 4: figures (a)–(d) show the relationship between voltages and currents of the circuits 1 and 2 w.r.t. time. Figure (e) shows the energy exchange between the two circuits. The coupling capacitor value is $C_c = 5.5$ μF.

more frequently as shown in figure 6(e). For the value of the coupling capacitor $C_c = 5.5$ μF, although the reduced model shows error as compared to the exact model, it shows better results in comparison with the Haus model.

Case 5: strongly coupled. Now we consider the set-up with the value of the coupling capacitor $C_c = 11$ μF, which is 50 percent of the value of the capacitor $C = 22$ μF; i.e. $\epsilon = 0.5$

In this case, figure 7 shows that the errors between the solutions of the exact model and the approximated models are increased. The solutions of the reduced model are not as good as those of the exact model, but they are better than those of the Haus model. In this case, the

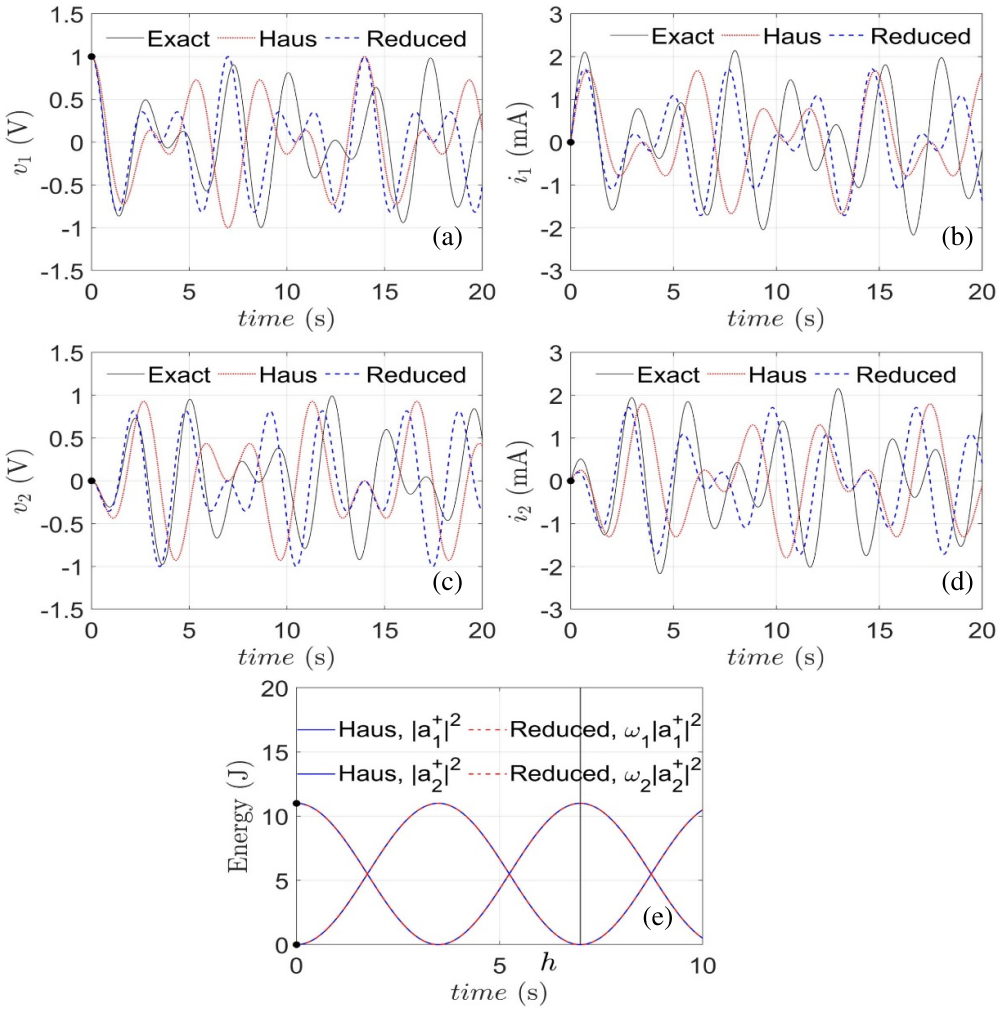

Figure 7. Case 5: figures (a)–(d) show the relationship between voltages and currents of the circuits 1 and 2 w.r.t. time. Figure (e) shows the energy exchange between the two circuits. The coupling capacitor value is $C_c = 11\ \mu$F.

phase and amplitude errors in the reduced model are small as compared to the Haus model in figures 7(a)–(d).

The reduced model and the Haus model show significant errors, and one has to use the 4×4 exact model for better accuracy. If the coupling is further increased, errors in both the approximation models become unacceptable, and one must use the exact model.

4.2. Coupling of non-identical oscillators

As explained in section (2.2), the Haus model is not applicable for the coupling set-up with non-identical oscillators. But here, one can use the proposed reduced model. In this section, we compare the performance of the reduced model with that of the exact model.

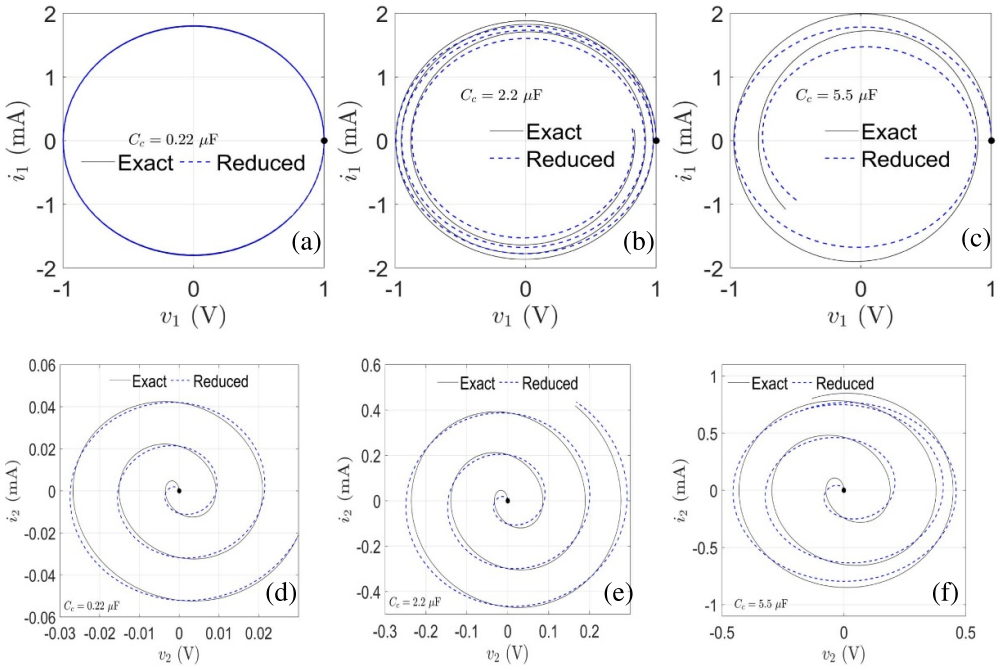

Figure 8. Non-identical coupling: figures (a)–(f) show the relationship between voltages and currents of the circuit 1 and 2 at different coupling capacitor value $C_c = 0.22(\epsilon = 0.01)$, $C_c = 2.2(\epsilon = 0.1)$, $C_c = 5.5(\epsilon = 0.25)$. Two non-identical LC circuits ($L_1 = 6.8\ \mu$H, $L_2 = 13.6\ \mu$H, $C_1 = 22\ \mu$F, $C_2 = 40.1\ \mu$F).

Here we consider two non-identical LC circuits with inductance value $L_1 = 6.8\ \mu$H, $L_2 = 13.6\ \mu$H and capacitance value $C_1 = 22\ \mu$F, $C_2 = 40.1\ \mu$H. The value of the coupling capacitor is increased relative to the value of the capacitor C_1. The initial condition for the exact model (32) and reduced model (35) is the same as in equation (43).

The relation between current and voltage of circuit 1 and circuit 2 at different coupling capacitor value $C_c = 0.22(\epsilon = 0.01)$, $C_c = 2.2(\epsilon = 0.1)$, $C_c = 5.5(\epsilon = 0.25)$ are shown in figure 8. For the case $\epsilon = 0.01$ and $\epsilon = 0.1$, the reduced model and exact model show similar results. Thus, the reduced model works for two weakly coupled non-identical LC circuits. However, as the coupling strengthens, one must use the exact model to analyze the dynamics faithfully.

5. Conclusions

In conclusion, this study focused on enhancing our understanding of the widely utilized Haus model, a time-domain phenomenological representation of the coupling between two oscillating systems. While the literature acknowledged the Haus model's applicability in weak coupling scenarios, a comprehensive analytical exploration of these approximations was lacking. This research aimed to bridge this gap by conducting a detailed analysis.

Although the discussions are centered around LC circuits for their simplicity, the analytical methods presented here can be applied to a broader range of coupled systems. Our investigation involved addressing the approximations in the Haus model and proposing improvements that extend its validity as a reduced-order model. By explicitly constructing the Hamiltonian, we

applied the analytical framework to coupled systems, emphasizing its versatility for various scenarios such as mass-spring systems or coupled pendulums.

By applying Hamiltonian and canonical transformation approaches, we derived a precise 4×4 system of differential equations describing the coupling between two LC circuits. Subsequently, we reduced this exact model to a more manageable 2×2 model, resembling the Haus model but with additional correction terms (i.e. self-coupling terms) in natural frequencies and exact coupling coefficients. Comparative analysis involving the Haus model, the reduced model, and the exact model demonstrated that, particularly in weak and moderately strong coupling scenarios, the reduced model outperformed the Haus model.

This research provided valuable insights into the accuracy of the approximated models by comparing their performance in terms of phase and amplitude errors. The findings revealed that the reduced model, despite being a first-order approximation like the Haus model, offered a more accurate solution. Overall, this work contributes to refining the understanding of the Haus model's limitations and the development of improved approximations for coupled oscillating systems.

This approach can be extended to time-domain studies of various oscillator coupling problems, such as coupled optical resonators or coupled mass-spring-like systems, etc. By first defining the system's Hamiltonian and identifying the appropriate canonical transformations, this method enables the derivation of self-coupling and (cross-)coupling coefficients, resulting in a more refined and accurate reduced model.

Data availability statement

No new data were created or analysed in this study.

Acknowledgments

Shubham Garg thanks the University Grant Commission (India) for the fellowship. The authors thank Prof. Deepakkumar Fulwani (Department of Electrical Engineering, IIT Jodhpur) and Prof. V Narayanan (Department of Physics, IIT Jodhpur) for fruitful discussions during this work. The authors are grateful to the anonymous reviewer for providing valuable comments that have improved the scope of the work.

ORCID iDs

Shubham Garg https://orcid.org/0000-0002-6520-5483
Kirankumar R Hiremath https://orcid.org/0000-0001-8393-2177

References

[1] Adato R, Artar A, Erramilli S and Altug H 2013 Engineered absorption enhancement and induced transparency in coupled molecular and plasmonic resonator systems *Nano Lett.* **13** 2584–91
[2] Agueev D and Pelinovsky D 2005 Modeling of wave resonances in low-contrast photonic crystals *SIAM J. Appl. Math.* **65** 1101–29
[3] Barclay P E, Srinivasan K and Painter O 2005 Nonlinear response of silicon photonic crystal microresonators excited via an integrated waveguide and fiber taper *Opt. Express* **13** 801–20
[4] Benzaouia M, Joannopoulos J D, Johnson S G and Karalis A 2021 Quasi-normal mode theory of the scattering matrix, enforcing fundamental constraints for truncated expansions *Phys. Rev. Res.* **3** 033228

[5] Bravo-Abad J, Fan S, Johnson S G, Joannopoulos J D and Soljacic M 2007 Modeling nonlinear optical phenomena in nanophotonics *J. Lightwave Technol.* **25** 2539–46
[6] Christopoulos T, Tsilipakos O and Kriezis E E 2024 Temporal coupled-mode theory in nonlinear resonant photonics: from basic principles to contemporary systems with 2D materials, dispersion, loss and gain *J. Appl. Phys.* **136** 011101
[7] Fan S 2002 Sharp asymmetric line shapes in side-coupled waveguide-cavity systems *Appl. Phys. Lett.* **80** 908–10
[8] Fan S 2008 Photonic crystal theory: temporal coupled-mode formalism *Optical Fiber Telecommunications V A* (Academic) pp 431–54
[9] Fan S, Suh W and Joannopoulos J D 2003 Temporal coupled-mode theory for the fano resonance in optical resonators *J. Opt. Soc. Am.* A **20** 569–72
[10] Ghatak A and Thyagarajan K 1989 *Optical Electronics* (Cambridge University Press)
[11] Gould R W 1955 A coupled mode description of the backward–wave oscillator and the Kompfner dip condition *IRE Trans. Electron Devices* **2** 37–42
[12] Hamill P 2014 *A Student's Guide to Lagrangians and Hamiltonians* (Cambridge University Press)
[13] Haus H 1984 *Waves and Fields in Optoelectronics* vol 402 (Prentice-Hall, Inc.)
[14] Haus H A and Huang W P 1991 Coupled mode theory *Proc. IEEE* **79** 1505–18
[15] Hu H, Shi Z, Zhang S and Xu H 2021 Unified treatment of scattering, absorption and luminescence spectra from a plasmon–exciton hybrid by temporal coupled-mode theory *J. Chem. Phys.* **155** 074104
[16] Joannopoulos J D, Johnson G G, Winn J N and Meade R D 2008 *Photonic Crystals: Molding the Flow of Light* (Princeton University Press)
[17] Lalanne P *et al* 2019 Quasinormal mode solvers for resonators with dispersive materials *J. Opt. Soc. Am.* A **36** 686–704
[18] Louisell W H 1955 Analysis of single tapered waveguide structure *Bell Syst. Tech. J.* **33** 853–70
[19] Louisell W H 1960 *Coupled Mode and Parametric Electronics* (Wiley)
[20] Manevitch L I and Musienko A I 2005 Short wavelength dynamics of the system of nonlinear oscillators coupled by stretched weightless beam *Chaos Solitons Fractals* **26** 107–16
[21] Martel C, Higuera M and Carrasco J 2009 Localized dispersive states in nonlinear coupled mode equations for light propagation in fiber Bragg gratings *SIAM J. Appl. Dyn. Syst.* **8** 576–91
[22] Miller S E 1954 Coupled wave theory and waveguide applications *Bell Syst. Tech. J.* **33** 661–719
[23] Panuluh A H 2020 The Lagrangian and Hamiltonian for RLC circuit: simple case *Int. J. Appl. Sci. Smart Technol.* **2** 169–78
[24] Pierce J R 1954 Coupling of modes of propagation *J. Appl. Phys.* **25** 179–83
[25] Shim H, Nam S and Lee B 2016 Time-domain analysis of wireless power transfer system behavior based on coupled-mode theory *J. Electromagn. Eng. Sci.* **16** 219–24
[26] Strogatz S H 2015 *Nonlinear Dynamics and Chaos: With Applications to Physics, Chemistry and Engineering* (CRC Press)
[27] Tao C, Zhu J, Zhong Y and Liu H 2020 Coupling theory of quasinormal modes for lossy and dispersive plasmonic nanoresonators *Phys. Rev.* B **102** 045430
[28] Timofeev I V, Pankin P S, Vetrov S Y, Arkhipkin V G, Lee W and Zyryanov V Y 2017 Chiral optical Tamm states: temporal coupled-mode theory *Crystals* **7** 113
[29] Wang K X 2018 Time-reversal symmetry in temporal coupled-mode theory and nonreciprocal device applications *Opt. Lett.* **43** 5623–6
[30] Xu H X, Ke L, Yang L and Qian J R 2011 Temporal coupled-mode theory for resonators *Proc. 2011 Cross Strait Quad-Regional Radio Science and Wireless Technology Conf.* vol 1 (IEEE) pp 82–84
[31] Yariv A 1973 Coupled-mode theory for guided-wave optics *IEEE J. Quantum Electron.* **9** 919–33
[32] Zhang H and Miller O D 2020 Quasinormal coupled mode theory (arXiv:2010.08650)
[33] Zhao Z, Guo C and Fan S 2019 Connection of temporal coupled-mode-theory formalisms for a resonant optical system and its time-reversal conjugate *Phys. Rev.* A **99** 033839